ASC Report No. 5/2010

Convergence of Adaptive FEM for some Elliptic Obstacle Problem

Marcus Page, Dirk Praetorius

Institute for Analysis and Scientific Computing
Vienna University of Technology — TU Wien
www.asc.tuwien.ac.at ISBN 978-3-902627-03-2

Most recent ASC Reports

4/2010 *Ansgar Jüngel, Josipa-Pina Milišić*
A Simplified Quantum Energy-Trans port Model for Semiconductors

3/2010 *Georg Kitzhofer, Othmar Koch, Gernot Pulverer, Christa Simon, Ewa Weinmüller*
The New MATLAB Code bvpsuite for the Solution of Singular Implicit BVPs

2/2010 *Maike Löhndorf, Jens Markus Melenk*
Wavenumber-explicit hp-BEM for High Frequency Scattering

1/2010 *Jens Markus Melenk*
Mapping Properties of Combined Field Helmholtz Boundary Integral Operators

49/2009 *Markus Aurada, Jens Markus Melenk, Dirk Praetorius*
Mixed Conforming Elements for the Large-Body Limit in Micromagnetics

48/2009 *Irene Reichl, Winfried Auzinger, Heinz-Bodo Schmiedmayer, Ewa Weinmüller*
Reconstructing the Knee Joint Mechanism from Kinematic Data

47/2009 *Irena Rachůnková, Svatoslav Staněk, Ewa Weinmüller, Michael Zenz*
Neumann Problems with Time Singularities

46/2009 *Kazuo Aoki, Ansgar Jüngel, Peter A. Markovich*
Small Velocity and finite Temperature Variations in Kinetic Relaxation Models

45/2009 *Ansgar Jüngel, Jan-Frederik Mennemann*
Time-dependent Simulations of Multidimensional Quantum Waveguides Using a Time-Splitting Spectral method

44/2009 *Markus Aurada, Michael Ebner, Samuel Ferraz-Leite, Petra Goldonits, Michael Karkulik, Markus Mayr, Dirk Praetorius*
HILBERT – A MATLAB Implementation of Adaptive BEM

Institute for Analysis and Scientific Computing
Vienna University of Technology
Wiedner Hauptstraße 8–10
1040 Wien, Austria

E-Mail: admin@asc.tuwien.ac.at
WWW: http://www.asc.tuwien.ac.at
FAX: +43-1-58801-10196

ISBN 978-3-902627-03-2

CONVERGENCE OF ADAPTIVE FEM FOR SOME ELLIPTIC OBSTACLE PROBLEM

M. PAGE AND D. PRAETORIUS

Abstract. In this work, we treat the convergence of adaptive lowest-order FEM for some elliptic obstacle problem with affine obstacle. For error estimation, we use a residual error estimator from [6]. We extend recent ideas from [12] for the unrestricted variational problem to overcome the lack of Galerkin orthogonality. The main result states that an appropriately weighted sum of energy error, edge residuals, and data oscillations satisfies a contraction property within each step of the adaptive feedback loop. This result is superior to a prior result from [6] in two ways: First, it is unnecessary to control the decay of the data oscillations explicitly. Second, our analysis avoids the use of a discrete local efficiency so that the local mesh-refinement is fairly arbitrary.

1. Introduction

1.1. Prior Work on Convergence of Adaptive FEM. Adaptive finite element methods for partial differential equations based on various types of a posteriori error estimators have been intensively studied and are now a standard tool in science and engineering, see e.g. the monographs [2, 23] and the references therein. As far as a posteriori error analysis for elliptic obstacle problems is concerned, we refer to [3, 5, 4, 13, 17, 20, 24].

In the case of elliptic boundary value problems, convergence of adaptive mesh-refining algorithms has first been proven in [14], followed by [18]. The latter works considered the residual error estimator for a P1-finite element discretization of the Poisson problem. In [18], the convergence analysis is based on reliability and the so-called *discrete local efficiency* of the residual error estimator, which relies on an *interior node property* for the local mesh-refinement. The main idea of the convergence proof then is to show that the error is contractive up to the data oscillations. This concept attracted quite some attention in the literature for various applications, e.g. the p-Laplacian [25], edge elements [8], mixed methods [9], nonconforming elements [10], and obstacle problems [6, 7].

For the Poisson problem, optimality of the adaptive algorithm from [18] was first shown in [22]. Recently, [12] presented a new convergence proof under weaker conditions. They showed that a weighted sum of error and error estimator satisfies a contraction property *without* requiring (discrete local) efficiency of the estimator. In particular, their proof avoided the interior node property of the local mesh-refinement, and they even proved optimality.

1.2. Contributions of Current Work. We consider the framework of [6], i.e. adaptive P1-finite elements for some elliptic obstacle problem with affine obstacle. However, to explain the differences to [6], we first recall their main result: Let $\varepsilon_\ell = \mathcal{J}(U_\ell) - \mathcal{J}(u) \geq 0$ denote the energy error, where u is the exact solution of the obstacle problem and U_ℓ is the finite

Date: February 8, 2010.

element approximation in the ℓ-th step of the adaptive algorithm. Based on a residual error estimator ϱ_ℓ consisting of edge jumps and inspired by [18], [6, Theorem 3] states that the ϱ_ℓ-steered adaptive mesh-refinement leads to

$$\varepsilon_{\ell+1} \le \kappa\, \varepsilon_\ell + C\, \mathrm{osc}_\ell^2 \quad \text{for all } \ell \in \mathbb{N},$$

with osc_ℓ being the data oscillations and with $0 < \kappa < 1$ and $C > 0$ being ℓ-independent constants. It is thus a consequence of elementary calculus that $\mathrm{osc}_\ell \to 0$ implies convergence $\varepsilon_\ell \to 0$ as $\ell \to \infty$. In [6, 18], however, the convergence $\mathrm{osc}_\ell \to 0$ of the data oscillations has to be guaranteed by the implementation.

The main ingredients of the proof of [6, Theorem 3] are the *reliability* of the error estimator, its *discrete local efficiency*, and the *marking strategy* introduced by Dörfler [14] ensuring an appropriate selection of edges and elements for refinement. The *discrete local efficiency*, however, strongly relies on the *interior node property* of the local mesh-refinement, and thus the validity of the convergence analysis is constrained by the refinement strategy.

We follow a different convergence approach, inspired by [12]: Our main result (Theorem 8, Corollary 9) states that the adaptive algorithm steered by $\eta_\ell^2 = \varrho_\ell^2 + \mathrm{osc}_\ell^2$, i.e. steered by edge jumps plus data oscillations, leads to

$$\Delta_{\ell+1} \le \kappa\, \Delta_\ell \quad \text{for all } \ell \in \mathbb{N}, \tag{1}$$

with a weighted sum $\Delta_\ell = \varepsilon_\ell + \gamma\, \mu_\ell^2$ and with $0 < \gamma, \kappa < 1$ being ℓ-independent constants. Here, μ_ℓ is a second error estimator introduced below which is equivalent to η_ℓ. Therefore, elementary calculus proves $\varepsilon_\ell \to 0$ as $\ell \to \infty$ without any further assumptions. Moreover, our result is fairly independent of the chosen mesh-refinement and does not need the *interior node property* as does the analysis of [6].

The first step for our proof of (1) is to observe that the Dörfler marking for η_ℓ implies the Dörfler marking for the auxiliary error estimator μ_ℓ. The latter is sufficient to show that the sequence of the estimators μ_ℓ is contractive in the sense that

$$\mu_{\ell+1}^2 \le q\, \mu_\ell^2 + C\, |||U_{\ell+1} - U_\ell|||^2 \quad \text{for all } \ell \in \mathbb{N}, \tag{2}$$

where $C > 0$ and $q \in (0,1)$ are certain ℓ-independent constants and $|||\cdot|||$ denotes the energy norm. To show this, we exploit the definition of the error estimator μ_ℓ, the marking strategy used, and basic properties of the local mesh-refinement. In addition and contrary to [12], our elementary analysis avoids to dominate the data oscillations osc_ℓ by the element residuals $\|h_\ell f\|_{L^2(\Omega)}$ and thus is slightly more accurate.

1.3. Outline of Current Work. In Section 2, we formulate the continuous and discrete obstacle problem, stated as energy minimization problems. Moreover, we recall the error estimator η_ℓ from [6] which is lateron used to steer our adaptive algorithm, and state its reliability (Proposition 2). In Section 3.1, we introduce an error estimator μ_ℓ which is equivalent to η_ℓ, namely

$$\eta_\ell \le \mu_\ell \le 4\, \eta_\ell. \tag{3}$$

We then recall the marking strategy and the local mesh-refinement used. As a consequence, we prove that the estimator μ_ℓ satisfies an estimator reduction property (Proposition 3), cf. (2). One major part of our proof is to show that the edge data oscillations are, in fact, contractive (Lemma 6). Finally, Section 3.2 states our version of the η_ℓ-steered adaptive mesh-refining algorithm (Algorithm 7) and proves the contraction result (1). In particular, the generated sequence of discrete solutions U_ℓ converges, in fact, to the continuous solution u (Theorem 8).

2. Model Problem

2.1. Continuous Formulation of Model Problem. Let Ω be a bounded domain in $\mathbb{R}^2$ with polygonal boundary $\Gamma := \partial\Omega$. We define an obstacle on $\overline{\Omega}$ by the affine function χ with $\chi \leq 0$ on $\partial\Omega$. By $\mathcal{A} \subset H_0^1(\Omega)$, we denote the set of admissible functions

$$\mathcal{A} = \big\{ v \in H_0^1(\Omega) \; : \; v \geq \chi \text{ a.e. in } \Omega \big\}, \tag{4}$$

which is convex, closed, and non-empty. For given $f \in L^2(\Omega)$, we consider the energy functional

$$\mathcal{J}(v) = \frac{1}{2} \langle\!\langle v \, , \, v \rangle\!\rangle - \langle f \, , \, v \rangle, \tag{5}$$

where the energy scalar product reads

$$\langle\!\langle u \, , \, v \rangle\!\rangle = \int_\Omega \nabla u \cdot \nabla v \, dx \quad \text{for all } u, v \in H_0^1(\Omega) \tag{6}$$

and where

$$\langle f \, , \, v \rangle = \int_\Omega f v \, dx \tag{7}$$

denotes the L^2-scalar product. By $|\!|\!| \cdot |\!|\!|$, we denote the energy norm on $H_0^1(\Omega)$ induced by $\langle\!\langle \cdot \, , \, \cdot \rangle\!\rangle$. The minimization problem then reads as follows: *Find $u \in \mathcal{A}$ such that*

$$\mathcal{J}(u) = \min_{v \in \mathcal{A}} \mathcal{J}(v). \tag{8}$$

The following well-known abstract lemma, found e.g. in [16, Theorem II.2.1], states unique solvability of this problem and equivalence to some variational inequality.

Lemma 1. *Let $\mathcal{H}$ be a Hilbert space over $\mathbb{R}$ with scalar product $\langle\!\langle \cdot \, , \, \cdot \rangle\!\rangle$ and induced norm $|\!|\!| \cdot |\!|\!|$. For any closed, convex, and non-empty subset $\mathcal{A}$ of $\mathcal{H}$ and any linear functional $f \in \mathcal{H}^*$, there is a unique minimizer $u \in \mathcal{A}$ of*

$$\mathcal{J}(u) = \min_{v \in \mathcal{A}} \mathcal{J}(v), \tag{9}$$

where the energy functional reads

$$\mathcal{J}(v) = \frac{1}{2} \langle\!\langle v \, , \, v \rangle\!\rangle - f(v). \tag{10}$$

This minimizer is equivalently characterized in terms of the following variational inequality: Find $u \in \mathcal{A}$ such that

$$\langle\!\langle u \, , \, u - v \rangle\!\rangle \leq f(u - v) \tag{11}$$

for all $v \in \mathcal{A}$. □

2.2. Conforming Discretization. For the numerical solution of (8), we consider conforming and shape regular triangulations $\mathcal{T}_\ell$ of Ω and denote the standard P1-finite element space of globally continuous and piecewise affine functions by $\mathcal{S}^1(\mathcal{T}_\ell)$. The finite dimensional minimization problem then reads as follows: *Find* $U_\ell \in \mathcal{A}_\ell := \mathcal{A} \cap \mathcal{S}^1(\mathcal{T}_\ell)$ *such that*

$$\mathcal{J}(U_\ell) = \min_{V_\ell \in \mathcal{A}} \mathcal{J}(V_\ell). \tag{12}$$

Note that $\mathcal{A}_\ell$ is a non-empty, convex, and closed subset of $\mathcal{S}^1(\mathcal{T}_\ell)$. With the same arguments as for the continuous problem, (12) admits a unique solution $U_\ell \in \mathcal{A}_\ell$.

Throughout all sections the set of all interior edges $E = T^+ \cap T^-$ for certain elements $T^+, T^- \in \mathcal{T}_\ell$ is denoted by $\mathcal{E}_\ell$. The set of all edges of $\mathcal{T}_\ell$ is denoted by $\mathcal{E}_\ell^\star$. In particular, $\mathcal{E}_{\ell,\Gamma} := \mathcal{E}_\ell^\star \backslash \mathcal{E}_\ell$ contains all boundary edges and provides some partition of Γ. Finally, $\mathcal{T}_{\ell,\Gamma} := \big\{T \in \mathcal{T}_\ell \,:\, T \cap \Gamma \neq \emptyset\big\}$ is the set of all elements which touch the boundary Γ.

2.3. Reliable Error Estimator. Now, let $u \in \mathcal{A}$ denote the continuous solution of (8) and $U_\ell \in \mathcal{A}_\ell$ be the discrete solution of (12) for some fixed triangulation $\mathcal{T}_\ell$. To steer the adaptive mesh-refinement, we use some residual-based error estimator

$$\eta_\ell^2 := \sum_{E \in \mathcal{E}_\ell} \big(\eta_\ell(E)^2 + \mathrm{osc}_\ell(E)^2\big) + \sum_{T \in \mathcal{T}_{\ell,\Gamma}} \mathrm{osc}_\ell(T)^2 \tag{13}$$

from [6]: First, $\eta_\ell(E)^2$ denotes the weighted L^2-norms of the normal jump

$$\eta_\ell(E)^2 := h_E \, \|[\partial_n U_\ell]\|_{L^2(E)}^2 \quad \text{for } E \in \mathcal{E}_\ell \tag{14}$$

with $h_E = \mathrm{diam}(E)$ the length of E and $[\cdot]$ the jump over an interior edge $E = T^+ \cap T^- \in \mathcal{E}_\ell$. Second, $\mathrm{osc}_\ell(E)^2$ denotes the data oscillations of f over E

$$\mathrm{osc}_\ell(E)^2 := |\Omega_{\ell,E}| \, \|f - f_{\Omega_{\ell,E}}\|_{L^2(\Omega_{\ell,E})}^2 \quad \text{for } E \in \mathcal{E}_\ell \tag{15}$$

with $\Omega_{\ell,E} = T^+ \cup T^-$ the patch associated with E and $f_{\Omega_{\ell,E}} = (1/|\Omega_{\ell,E}|) \int_{\Omega_{\ell,E}} f \, dx$ the corresponding integral mean of f. Finally, for elements $T \in \mathcal{T}_{\ell,\Gamma}$ at the boundary, η_ℓ involves the weighted element residuals

$$\mathrm{osc}_\ell(T)^2 := |T| \|f\|_{L^2(T)}^2 \quad \text{for } T \in \mathcal{T}_\ell. \tag{16}$$

The following proposition has essentially been shown in [6], where $\mathrm{osc}_\ell(T)$ is, however, weighted by $\mathrm{diam}(T)^2 \sim |T|$. We will discuss this, up to shape regularity, equivalent definition lateron, cf. Corollary 9 in Section 3.2.

Proposition 2. *The estimator* η_ℓ *from* (13) *is reliable in the sense that there holds*

$$\frac{1}{2} \, |||u - U_\ell|||^2 \le \mathcal{J}(U_\ell) - \mathcal{J}(u) \le C_1 \, \eta_\ell^2. \tag{17}$$

The constant $C_1 > 0$ *depends only on* Ω *and the shape of the elements in* $\mathcal{T}_\ell$.

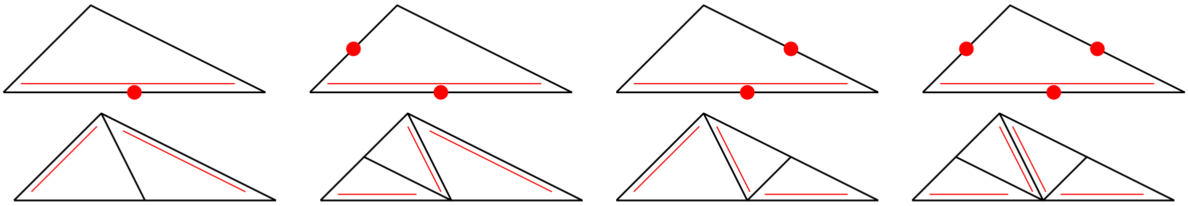

FIGURE 1. For each triangle $T \in \mathcal{T}$, there is one fixed *reference edge*, indicated by the double line (left, top). Refinement of T is done by bisecting the reference edge, where its midpoint becomes a new node. The reference edges of the son triangles are opposite to this newest vertex (left, bottom). To avoid hanging nodes, one proceeds as follows: We assume that certain edges of T, but at least the reference edge, are marked for refinement (top). Using iterated newest vertex bisection, the element is then split into 2, 3, or 4 son triangles (bottom).

Proof. The upper bound is stated in [6, Theorem 1]. To see the lower bound, we use the variational inequality (11). For $v = U_\ell$, this gives

$$\begin{aligned}
|||u - U_\ell|||^2 &= \langle\!\langle u\,,\,u - U_\ell\rangle\!\rangle + |||U_\ell|||^2 - \langle\!\langle U_\ell\,,\,u\rangle\!\rangle \\
&\le \Big(\frac{1}{2}|||U_\ell|||^2 - \langle f\,,\,U_\ell\rangle\Big) - \Big(\frac{1}{2}\,|||u|||^2 - \langle f\,,\,u\rangle\Big) \\
&\quad + \Big(\frac{1}{2}\,|||U_\ell|||^2 - \langle\!\langle U_\ell\,,\,u\rangle\!\rangle + \frac{1}{2}\,|||u|||^2\Big) \\
&= \mathcal{J}(U_\ell) - \mathcal{J}(u) + \frac{1}{2}\,|||u - U_\ell|||^2
\end{aligned}$$

and concludes the proof. $\square$

3. A Convergent Adaptive Algorithm

3.1. Estimator Reduction. First, we define a slight modification of the error estimator η_ℓ introduced above. Recall that $\mathcal{E}_\ell^\star$ is the set of all edges of $\mathcal{T}_\ell$. For the interior edges $E \in \mathcal{E}_\ell$, the edge data oscillations $\mathrm{osc}_\ell(E)$ are defined in (15). For the boundary edges, we define

$$\mathrm{osc}_\ell(E)^2 := \mathrm{osc}_\ell(T)^2 \quad \text{for all } E \in \mathcal{E}_{\ell,\Gamma} := \mathcal{E}_\ell^\star \backslash \mathcal{E}_\ell \text{ and } T \in \mathcal{T}_{\ell,\Gamma} \text{ with } E \subset \partial T, \tag{18}$$

where $\mathrm{osc}_\ell(T)$ is defined in (16). We now consider

$$\mu_\ell^2 := \sum_{E\in\mathcal{E}_\ell} \eta_\ell(E)^2 + \sum_{E\in\mathcal{E}_\ell^\star} \mathrm{osc}_\ell(E)^2 + \sum_{T\in\mathcal{T}_{\ell,\Gamma}} \mathrm{osc}_\ell(T)^2. \tag{19}$$

By definition, there holds

$$\eta_\ell^2 \le \mu_\ell^2 \le 4\,\eta_\ell^2, \tag{20}$$

since one element $T \in \mathcal{T}_{\ell,\Gamma}$ may have at most three boundary edges. In particular, this proves that the reliability estimate (17) also holds with η_ℓ replaced by μ_ℓ.

For the moment, let us use the local contributions of μ_ℓ to steer some adaptive mesh-refining algorithm. For marking, we use the marking strategy introduced by Dörfler [14]. Contrary to [14, 18] and [6], we use $\mathcal{E}_\ell^\star \cup \mathcal{T}_{\ell,\Gamma}$ as index set for the marking criterion instead of only $\mathcal{E}_\ell$, and we mark simultaneously for $\eta_\ell(E)$ and data oscillations $\mathrm{osc}_\ell(E)$ resp. $\mathrm{osc}_\ell(T)$:

Given some parameter $\theta \in (0,1)$, we seek a set $\mathcal{M}_\ell \subseteq \mathcal{E}_\ell^\star \cup \mathcal{T}_{\ell,\Gamma}$ of usually minimal cardinality such that

$$\theta\,\mu_\ell^2 \le \sum_{E\in\mathcal{E}_\ell\cap\mathcal{M}_\ell} \eta_\ell(E)^2 + \sum_{E\in\mathcal{E}_\ell^\star\cap\mathcal{M}_\ell} \mathrm{osc}_\ell(E)^2 + \sum_{T\in\mathcal{T}_{\ell,\Gamma}\cap\mathcal{M}_\ell} \mathrm{osc}_\ell(T)^2. \tag{21}$$

For the mesh-refinement, we use newest-vertex bisection, where we mark all edges $E \in \mathcal{E}_\ell^\star \cap \mathcal{M}_\ell$ for refinement. For all elements $T \in \mathcal{T}_{\ell,\Gamma} \cap \mathcal{M}_\ell$, we mark their reference edge. The refinement rules are shown in Figure 1, and the reader is also referred to [23, Chapter 4]. Besides uniform shape regularity of $\mathcal{T}_{\ell+1}$, there is a certain decay of the mesh-widths:

- Marked edges $E \in \mathcal{M}_\ell$ are split into two edges $E', E'' \in \mathcal{E}_{\ell+1}^\star$ of half length.
- If at least one edge E of an element $T \in \mathcal{T}_\ell$ is marked, T is refined into up to four son elements $T' \in \mathcal{T}_{\ell+1}$ with $|T|/4 \le |T'| \le |T|/2$, cf. Figure 1.

These observations are essential to prove the following result.

Proposition 3. *Suppose that the set $\mathcal{M}_\ell \subseteq \mathcal{E}_\ell^\star \cup \mathcal{T}_{\ell,\Gamma}$ satisfies (21) and that marked edges and marked elements are refined as stated before. Then, there holds*

$$\mu_{\ell+1}^2 \le q\,\mu_\ell^2 + C_2 |||U_{\ell+1} - U_\ell|||^2 \tag{22}$$

with some contraction constant $q \in (0,1)$ which depends only on $\theta \in (0,1)$. The constant $C_2 > 0$ additionally depends on the shape of the elements in $\mathcal{T}_0$.

For the convenience of the reader, the proof of Proposition 3 is split into three lemmata which estimate the decay of the different contributions of μ_ℓ if the mesh $\mathcal{T}_\ell$ is locally refined.

Lemma 4. *According to the refinement of marked elements $T \in \mathcal{T}_{\ell,\Gamma} \cap \mathcal{M}_\ell$, there holds*

$$\sum_{T'\in\mathcal{T}_{\ell+1,\Gamma}} \mathrm{osc}_{\ell+1}(T')^2 \le \sum_{T\in\mathcal{T}_{\ell,\Gamma}} \mathrm{osc}_\ell(T)^2 - \frac{1}{2} \sum_{T\in\mathcal{T}_{\ell,\Gamma}\cap\mathcal{M}_\ell} \mathrm{osc}_\ell(T)^2. \tag{23}$$

Proof. We define the set $\overline{\mathcal{M}}_{\mathcal{T},\ell} := \big\{T' \in \mathcal{T}_{\ell+1} \,:\, \exists T \in \mathcal{T}_{\ell,\Gamma} \cap \mathcal{M}_\ell \quad T' \subseteq T\big\}$ containing all elements obtained by refinement of marked elements. Then,

$$\begin{aligned}
\sum_{T'\in\mathcal{T}_{\ell+1,\Gamma}} \mathrm{osc}_{\ell+1}(T')^2 &\le \sum_{T'\in\mathcal{T}_{\ell+1,\Gamma}\setminus\overline{\mathcal{M}}_{\mathcal{T},\ell}} |T'|\|f\|_{L^2(T')}^2 + \sum_{T'\in\overline{\mathcal{M}}_{\mathcal{T},\ell}} |T'|\|f\|_{L^2(T')}^2 \\
&\le \sum_{T\in\mathcal{T}_{\ell,\Gamma}\setminus\mathcal{M}_\ell} |T|\|f\|_{L^2(T)}^2 + \frac{1}{2} \sum_{T\in\mathcal{T}_{\ell,\Gamma}\cap\mathcal{M}_\ell} |T|\|f\|_{L^2(T)}^2 \\
&= \sum_{T\in\mathcal{T}_{\ell,\Gamma}\setminus\mathcal{M}_\ell} \mathrm{osc}_\ell(T)^2 + \frac{1}{2} \sum_{T\in\mathcal{T}_{\ell,\Gamma}\cap\mathcal{M}_\ell} \mathrm{osc}_\ell(T)^2,
\end{aligned}$$

where we have used that each father $T \in \mathcal{T}_\ell$ is the disjoint union of its sons $T' \in \mathcal{T}_{\ell+1}$. ☐

Lemma 5. *According to the refinement of marked edges $E \in \mathcal{E}_\ell \cap \mathcal{M}_\ell$, there holds*

$$\sum_{E'\in\mathcal{E}_{\ell+1}} h_{E'}\,\|[\partial_n U_\ell]\|_{L^2(E')}^2 \le \sum_{E\in\mathcal{E}_\ell} \eta_\ell(E)^2 - \frac{1}{2} \sum_{E\in\mathcal{E}_\ell\cap\mathcal{M}_\ell} \eta_\ell(E)^2, \tag{24}$$

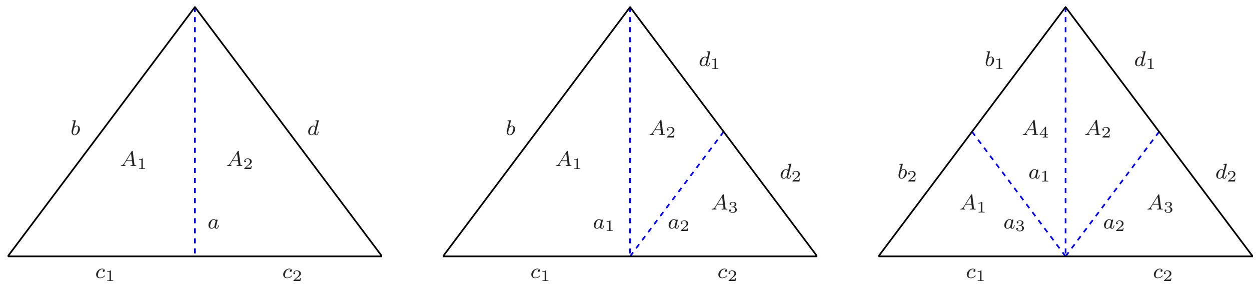

FIGURE 2. Refinement of an element A by one (left), two (middle), or three (right) bisections and notation used in the proof of Lemma 6.

Proof. We define the set $\overline{\mathcal{M}}_{\mathcal{E},\ell} := \big\{E' \in \mathcal{E}_{\ell+1} \,:\, \exists E \in \mathcal{E}_\ell \cap \mathcal{M}_\ell \quad E' \subseteq E\big\}$ containing all edges obtained by refinement of marked edges. Then, one observes

$$\begin{aligned}\sum_{E' \in \mathcal{E}_{\ell+1}} h_{E'} \, \|[\partial_n U_\ell]\|^2_{L^2(E')} &= \sum_{E' \in \mathcal{E}_{\ell+1} \setminus \overline{\mathcal{M}}_{\mathcal{E},\ell}} h_{E'} \, \|[\partial_n U_\ell]\|^2_{L^2(E')} + \sum_{E' \in \overline{\mathcal{M}}_{\mathcal{E},\ell}} h_{E'} \, \|[\partial_n U_\ell]\|^2_{L^2(E')} \\ &\le \sum_{E \in \mathcal{E}_\ell \setminus \mathcal{M}_\ell} h_E \, \|[\partial_n U_\ell]\|^2_{L^2(E)} + \frac{1}{2} \sum_{E \in \mathcal{E}_\ell \cap \mathcal{M}_\ell} h_E \, \|[\partial_n U_\ell]\|^2_{L^2(E)} \\ &= \sum_{E \in \mathcal{E}_\ell \setminus \mathcal{M}_\ell} \eta_\ell(E)^2 + \frac{1}{2} \sum_{E \in \mathcal{E}_\ell \cap \mathcal{M}_\ell} \eta_\ell(E)^2,\end{aligned}$$

where we have used that the jump $[\partial_n U_\ell]$ is zero on all edges $E' \in \mathcal{E}_{\ell+1}$ which lie inside an element $T \in \mathcal{T}_\ell$. $\square$

Lemma 6. *According to the refinement of marked edges $E \in \mathcal{E}_\ell^\star \cap \mathcal{M}_\ell$, there holds*

$$\sum_{E' \in \mathcal{E}_{\ell+1}^\star} \mathrm{osc}_{\ell+1}(E')^2 \le \sum_{E \in \mathcal{E}_\ell^\star} \mathrm{osc}_\ell(E)^2 - \frac{1}{4} \sum_{E \in \mathcal{E}_\ell^\star \cap \mathcal{M}_\ell} \mathrm{osc}_\ell(E)^2. \tag{25}$$

Proof. The proof of (25) is considerably longer than for the prior contributions in (23)–(24). The reason is that local mesh-refinement leads to additional edges inside of refined elements $T \in \mathcal{T}_\ell$. This provides additional contributions which have to be controlled. To that end, we define for any edge $E \in \mathcal{E}_{\ell+1}^\star$ and any element $T \in \mathcal{T}_\ell$ with $|T \cap \Omega_{\ell+1,E}| > 0$ the quantity

$$\mathrm{osc}_{\ell+1}(E|T)^2 = |\Omega_{\ell+1,E}| \, \|f - f_{\Omega_{\ell+1,E}}\|^2_{L^2(\Omega_{\ell+1,E} \cap T)},$$

where we let $\Omega_{\ell+1,E} := T'$ and $f_{\Omega_{\ell+1,E}} := 0$ for a boundary edge $E \in \mathcal{E}_{\ell+1,\Gamma} = \mathcal{E}_{\ell+1}^\star \setminus \mathcal{E}_{\ell+1}$ and $T' \in \mathcal{T}_{\ell+1,\Gamma}$ the unique element with $E \subset \partial T'$. Throughout the proof, $f_\omega = (1/|\omega|) \int_\omega f \, dx$ denotes the integral mean of f over the measurable set ω. Note that the L^2-best approximation property of f_ω yields

$$\|f - f_\omega\|_{L^2(\omega)} \le \|f - \alpha\|_{L^2(\omega)} \quad \text{for all } \alpha \in \mathbb{R},$$

whence

$$\|f - f_\omega\|_{L^2(\omega)} \le \|f - f_{\widehat{\omega}}\|_{L^2(\widehat{\omega})} \quad \text{for all measurable sets } \widehat{\omega} \supset \omega.$$

For each element $A \in \mathcal{T}_\ell$, only four cases occur: A is either not refined, i.e. $A \in \mathcal{T}_\ell \cap \mathcal{T}_{\ell+1}$, or refined by either one, two, or three bisections, cf. Figure 2.

First, assume that an element $A \in \mathcal{T}_\ell \cap \mathcal{T}_{\ell+1}$ is not refined. Let $b, c, d \in \mathcal{E}_\ell \cap \mathcal{E}_{\ell+1}$ denote its three edges. We then define

$$o_\ell(b|A)^2 = \mathrm{osc}_{\ell+1}(b|A)^2, \quad o_\ell(c|A)^2 = \mathrm{osc}_{\ell+1}(c|A)^2, \quad \text{and} \quad o_\ell(d|A)^2 = \mathrm{osc}_{\ell+1}(d|A)^2.$$

By definition, we obtain

$$\sum_{\substack{E \in \mathcal{E}^\star_{\ell+1} \\ |A \cap \Omega_{\ell+1,E}|>0}} \mathrm{osc}_{\ell+1}(E|A)^2 \le \sum_{\substack{E \in \mathcal{E}^\star_\ell \\ E \subset \partial A}} o_\ell(E|A)^2 \tag{26}$$

even with equality.

Second, assume that an element $A \in \mathcal{T}_\ell$ with edges $b, c, d \in \mathcal{E}^\star_\ell$ is refined by one bisection, cf. Figure 2, where the edge c is split into $c_1, c_2 \in \mathcal{E}^\star_{\ell+1}$ and where one additional edge $a \in \mathcal{E}^\star_{\ell+1}$ is created. Moreover, A is split into elements $A_1, A_2 \in \mathcal{T}_{\ell+1}$ with area $|A_1| = |A_2| = |A|/2$. Let $B, C, D \in \mathcal{T}_\ell$ be the neighbours of A along the edges $b, c, d \in \mathcal{E}^\star_\ell$, where for instance $B = \emptyset$ if $b \in \mathcal{E}^\star_\ell \backslash \mathcal{E}_\ell$ is a boundary edge. Then,

$$\begin{aligned}
&\sum_{\substack{E \in \mathcal{E}^\star_{\ell+1} \\ |A \cap \Omega_{\ell+1,E}|>0}} \mathrm{osc}_{\ell+1}(E|A)^2 \\
&\quad = \mathrm{osc}_{\ell+1}(c_1|A)^2 + \mathrm{osc}_{\ell+1}(c_2|A)^2 + \mathrm{osc}_{\ell+1}(b|A)^2 + \mathrm{osc}_{\ell+1}(d|A)^2 + \mathrm{osc}_{\ell+1}(a|A)^2 \\
&\quad = \big(|\Omega_{\ell+1,c_1} \cap C| + |A|/2\big) \, \|f - f_{\Omega_{\ell+1,c_1}}\|^2_{L^2(A_1)} + \big(|\Omega_{\ell+1,c_2} \cap C| + |A|/2\big) \, \|f - f_{\Omega_{\ell+1,c_2}}\|^2_{L^2(A_2)} \\
&\qquad + \big(|\Omega_{\ell+1,b} \cap B| + |A|/2\big) \, \|f - f_{\Omega_{\ell+1,b}}\|^2_{L^2(A_1)} + \big(|\Omega_{\ell+1,d} \cap D| + |A|/2\big) \, \|f - f_{\Omega_{\ell+1,d}}\|^2_{L^2(A_2)} \\
&\qquad + |A| \, \|f - f_A\|^2_{L^2(A)}.
\end{aligned}$$

The last term belongs to the new edge $a \in \mathcal{E}^\star_{\ell+1}$. We define

$$\begin{aligned}
o_\ell(b|A)^2 &= \big(|\Omega_{\ell+1,b} \cap B| + |A|/2\big) \, \|f - f_{\Omega_{\ell+1,b}}\|^2_{L^2(A_1)} + (|A|/2) \, \|f - f_A\|^2_{L^2(A)}, \\
o_\ell(c|A)^2 &= \big(|\Omega_{\ell+1,c_1} \cap C| + |A|/2\big) \, \|f - f_{\Omega_{\ell+1,c_1}}\|^2_{L^2(A_1)} \\
&\quad + \big(|\Omega_{\ell+1,c_2} \cap C| + |A|/2\big) \, \|f - f_{\Omega_{\ell+1,c_2}}\|^2_{L^2(A_2)}, \\
o_\ell(d|A)^2 &= \big(|\Omega_{\ell+1,d} \cap D| + |A|/2\big) \, \|f - f_{\Omega_{\ell+1,d}}\|^2_{L^2(A_2)} + (|A|/2) \, \|f - f_A\|^2_{L^2(A)}
\end{aligned}$$

and observe that, by definition, (26) holds with equality.

Third, assume that an element $A \in \mathcal{T}_\ell$ with edges $b, c, d \in \mathcal{E}^\star_\ell$ is refined by two bisections, cf. Figure 2, where the edges c, d are split into $c_1, c_2, d_1, d_2 \in \mathcal{E}^\star_{\ell+1}$, respectively, and two new edges $a_1, a_2 \in \mathcal{E}^\star_{\ell+1}$ are created. Moreover, A is split into elements $A_1, A_2, A_3 \in \mathcal{T}_{\ell+1}$ with area $|A_1| = |A|/2$ and $|A_2| = |A_3| = |A|/4$. Let b, c, d and B, C, D be the same as in the previous case. Then,

$$
\begin{aligned}
&\sum_{\substack{E\in\mathcal{E}^\star_{\ell+1}\\|A\cap\Omega_{\ell+1,E}|>0}} \mathrm{osc}_{\ell+1}(E|A)^2\\
&\quad= \mathrm{osc}_{\ell+1}(c_1|A)^2 + \mathrm{osc}_{\ell+1}(c_2|A)^2 + \mathrm{osc}_{\ell+1}(d_1|A)^2 + \mathrm{osc}_{\ell+1}(d_2|A)^2 + \mathrm{osc}_{\ell+1}(b|A)^2\\
&\qquad + \mathrm{osc}_{\ell+1}(a_1|A)^2 + \mathrm{osc}_{\ell+1}(a_2|A)^2\\
&\quad= \big(|\Omega_{\ell+1,c_1}\cap C| + |A|/2\big)\,\|f - f_{\Omega_{\ell+1,c_1}}\|^2_{L^2(A_1)} + \big(|\Omega_{\ell+1,c_2}\cap C| + |A|/4\big)\,\|f - f_{\Omega_{\ell+1,c_2}}\|^2_{L^2(A_3)}\\
&\qquad + \big(|\Omega_{\ell+1,d_1}\cap D| + |A|/4\big)\,\|f - f_{\Omega_{\ell+1,d_1}}\|^2_{L^2(A_2)} + \big(|\Omega_{\ell+1,d_2}\cap D| + |A|/4\big)\,\|f - f_{\Omega_{\ell+1,d_2}}\|^2_{L^2(A_3)}\\
&\qquad + \big(|\Omega_{\ell+1,b}\cap B| + |A|/2\big)\,\|f - f_{\Omega_{\ell+1,b}}\|^2_{L^2(A_1)}\\
&\qquad + (3|A|/4)\,\|f - f_{A_1\cup A_2}\|^2_{L^2(A_1\cup A_2)} + (|A|/2)\,\|f - f_{A_2\cup A_3}\|^2_{L^2(A_2\cup A_3)}.
\end{aligned}
$$

The last two terms belong to the new edges $a_1, a_2 \in \mathcal{E}^\star_{\ell+1}$ and are roughly estimated by

$$
(3|A|/4)\,\|f - f_{A_1\cup A_2}\|^2_{L^2(A_1\cup A_2)} + (|A|/2)\,\|f - f_{A_2\cup A_3}\|^2_{L^2(A_2\cup A_3)} \le (5|A|/4)\,\|f - f_A\|^2_{L^2(A)}.
$$

We define

$$
\begin{aligned}
o_\ell(b|A)^2 &= \big(|\Omega_{\ell+1,b}\cap B| + |A|/2\big)\,\|f - f_{\Omega_{\ell+1,b}}\|^2_{L^2(A_1)} + (|A|/2)\,\|f - f_A\|^2_{L^2(A)},\\
o_\ell(c|A)^2 &= \big(|\Omega_{\ell+1,c_1}\cap C| + |A|/2\big)\,\|f - f_{\Omega_{\ell+1,c_1}}\|^2_{L^2(A_1)}\\
&\qquad + \big(|\Omega_{\ell+1,c_2}\cap C| + |A|/4\big)\,\|f - f_{\Omega_{\ell+1,c_2}}\|^2_{L^2(A_3)} + (|A|/4)\,\|f - f_A\|^2_{L^2(A)},\\
o_\ell(d|A)^2 &= \big(|\Omega_{\ell+1,d_1}\cap D| + |A|/4\big)\,\|f - f_{\Omega_{\ell+1,d_1}}\|^2_{L^2(A_2)}\\
&\qquad + \big(|\Omega_{\ell+1,d_2}\cap D| + |A|/4\big)\,\|f - f_{\Omega_{\ell+1,d_2}}\|^2_{L^2(A_3)} + (|A|/2)\,\|f - f_A\|^2_{L^2(A)}.
\end{aligned}
$$

By definition, we again obtain (26).

Fourth, assume that an element $A \in \mathcal{T}_\ell$ with edges $b, c, d \in \mathcal{E}^\star_\ell$ is refined by three bisections, cf. Figure 2, where the edges b, c, d are split into $b_1, b_2, c_1, c_2, d_1, d_2 \in \mathcal{E}^\star_{\ell+1}$, respectively, and three new edges $a_1, a_2, a_3 \in \mathcal{E}^\star_{\ell+1}$ are created. Moreover, A is split into elements $A_1, A_2, A_3, A_4 \in \mathcal{T}_{\ell+1}$ with area $|A_j| = |A|/4$. For b, c, d and B, C, D, we use the notation from the previous cases. Then,

$$
\begin{aligned}
&\sum_{\substack{E\in\mathcal{E}^\star_{\ell+1}\\|A\cap\Omega_{\ell+1,E}|>0}} \mathrm{osc}_{\ell+1}(E|A)^2\\
&\quad= \mathrm{osc}_{\ell+1}(b_1|A)^2 + \mathrm{osc}_{\ell+1}(b_2|A)^2 + \mathrm{osc}_{\ell+1}(c_1|A)^2 + \mathrm{osc}_{\ell+1}(c_2|A)^2\\
&\qquad + \mathrm{osc}_{\ell+1}(d_1|A)^2 + \mathrm{osc}_{\ell+1}(d_2|A)^2 + \mathrm{osc}_{\ell+1}(a_1|A)^2 + \mathrm{osc}_{\ell+1}(a_2|A)^2 + \mathrm{osc}_{\ell+1}(a_3|A)^2\\
&\quad\le \big(|\Omega_{\ell+1,b_1}\cap B| + |A|/4\big)\,\|f - f_{\Omega_{\ell+1,b_1}}\|^2_{L^2(A_4)} + \big(|\Omega_{\ell+1,b_2}\cap B| + |A|/4\big)\,\|f - f_{\Omega_{\ell+1,b_2}}\|^2_{L^2(A_1)}\\
&\qquad + \big(|\Omega_{\ell+1,c_1}\cap C| + |A|/4\big)\,\|f - f_{\Omega_{\ell+1,c_1}}\|^2_{L^2(A_1)} + \big(|\Omega_{\ell+1,c_2}\cap C| + |A|/4\big)\,\|f - f_{\Omega_{\ell+1,c_2}}\|^2_{L^2(A_3)}\\
&\qquad + \big(|\Omega_{\ell+1,d_1}\cap D| + |A|/4\big)\,\|f - f_{\Omega_{\ell+1,d_1}}\|^2_{L^2(A_2)} + \big(|\Omega_{\ell+1,d_2}\cap D| + |A|/4\big)\,\|f - f_{\Omega_{\ell+1,d_2}}\|^2_{L^2(A_3)}\\
&\qquad + (3|A|/2)\,\|f - f_A\|^2_{L^2(A)}.
\end{aligned}
$$

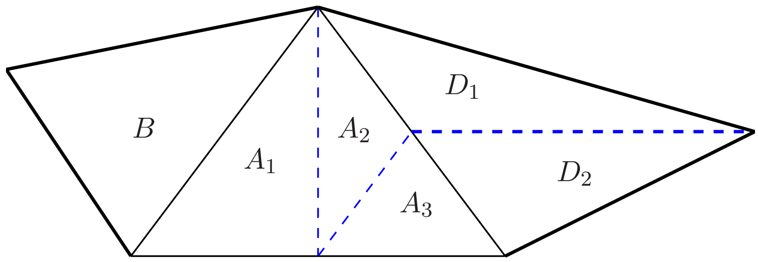

FIGURE 3. The element $A \in \mathcal{T}_\ell$ is refined by two bisections. It has two neighbouring elements $B, D \in \mathcal{T}_\ell$, whereas the third edge is on the boundary.

Defining

$$
\begin{aligned}
o_\ell(b|A)^2 &= \big(|\Omega_{\ell+1,b_1} \cap B| + |A|/4\big)\, \|f - f_{\Omega_{\ell+1,b_1}}\|^2_{L^2(A_4)} \\
&\qquad + \big(|\Omega_{\ell+1,b_2} \cap B| + |A|/4\big)\, \|f - f_{\Omega_{\ell+1,b_2}}\|^2_{L^2(A_1)} + (|A|/2)\, \|f - f_A\|^2_{L^2(A)} \\
o_\ell(c|A)^2 &= \big(|\Omega_{\ell+1,c_1} \cap C| + |A|/4\big)\, \|f - f_{\Omega_{\ell+1,c_1}}\|^2_{L^2(A_1)} \\
&\qquad + \big(|\Omega_{\ell+1,c_2} \cap C| + |A|/4\big)\, \|f - f_{\Omega_{\ell+1,c_2}}\|^2_{L^2(A_3)} + (|A|/2)\, \|f - f_A\|^2_{L^2(A)} \\
o_\ell(d|A)^2 &= \big(|\Omega_{\ell+1,d_1} \cap D| + |A|/4\big)\, \|f - f_{\Omega_{\ell+1,d_1}}\|^2_{L^2(A_2)} \\
&\qquad + \big(|\Omega_{\ell+1,d_2} \cap D| + |A|/4\big)\, \|f - f_{\Omega_{\ell+1,d_2}}\|^2_{L^2(A_3)} + (|A|/2)\, \|f - f_A\|^2_{L^2(A)},
\end{aligned}
$$

we again guarantee (26).

Now, it only remains to show that for non-refined edges holds

$$
\sum_{\substack{T \in \mathcal{T}_\ell \\ T \subset \Omega_{\ell,E}}} o_\ell(E|T)^2 \le \mathrm{osc}_\ell(E)^2 \quad \text{for all } E \in \mathcal{E}^\star_\ell \cap \mathcal{E}^\star_{\ell+1}, \tag{27}
$$

whereas for edges which are refined, there holds

$$
\sum_{\substack{T \in \mathcal{T}_\ell \\ T \subset \Omega_{\ell,E}}} o_\ell(E|T)^2 \le \frac{3}{4}\, \mathrm{osc}_\ell(E)^2 \quad \text{for all } E \in \mathcal{E}^\star_\ell \backslash \mathcal{E}^\star_{\ell+1}. \tag{28}
$$

Of course, there are quite some cases to be considered. Since all follow by direct calculation, we only consider some particular examples shown in Figure 3, while we refer to [21] for the consideration of all possible cases.

We first consider $b := A \cap B \in \mathcal{E}_\ell$. According to our definitions, there holds

$$
\begin{aligned}
o_\ell(b|B)^2 &= \big(|A|/2 + |B|\big)\, \|f - f_{A_1 \cup B}\|^2_{L^2(B)}, \\
o_\ell(b|A)^2 &= \big(|B| + |A|/2\big)\, \|f - f_{A_1 \cup B}\|^2_{L^2(A_1)} + (|A|/2)\, \|f - f_A\|^2_{L^2(A)}.
\end{aligned}
$$

This implies

$$
\begin{aligned}
o_\ell(b|A)^2 + o_\ell(b|B)^2 &= \big(|A|/2 + |B|\big)\, \|f - f_{A_1 \cup B}\|^2_{L^2(A_1 \cup B)} + (|A|/2)\, \|f - f_A\|^2_{L^2(A)} \\
&\le \big(|A|/2 + |B|\big)\, \|f - f_{A \cup B}\|^2_{L^2(A \cup B)} + (|A|/2)\, \|f - f_{A \cup B}\|^2_{L^2(A \cup B)} \\
&= \mathrm{osc}_\ell(b)^2.
\end{aligned}
$$

Next, we consider $d := A \cap D \in \mathcal{E}_\ell$. We have

$$\begin{aligned}
o_\ell(d|D)^2 &= \big(|A|/4 + |D|/2\big)\, \|f - f_{A_2 \cup D_1}\|^2_{L^2(D_1)} + \big(|A|/4 + |D|/2\big)\, \|f - f_{A_3 \cup D_2}\|^2_{L^2(D_2)}, \\
o_\ell(d|A)^2 &= \big(|D|/2 + |A|/4\big)\, \|f - f_{A_2 \cup D_1}\|^2_{L^2(A_2)} + \big(|D|/2 + |A|/4\big)\, \|f - f_{A_3 \cup D_2}\|^2_{L^2(A_3)} \\
&\qquad + (|A|/2)\, \|f - f_A\|^2_{L^2(A)}.
\end{aligned}$$

This implies

$$\begin{aligned}
o_\ell(d|A)^2 + o_\ell(d|B)^2 &= \big(|A|/4 + |D|/2\big)\, \|f - f_{A_2 \cup D_1}\|^2_{L^2(A_2 \cup D_1)} \\
&\qquad + \big(|A|/4 + |D|/2\big)\, \|f - f_{A_3 \cup D_2}\|^2_{L^2(A_3 \cup D_2)} + (|A|/2)\, \|f - f_A\|^2_{L^2(A)} \\
&\le \big(|A|/4 + |D|/2\big)\, \|f - f_{A \cup D}\|^2_{L^2(A \cup D)} + (|A|/2)\, \|f - f_{A \cup D}\|^2_{L^2(A)} \\
&\le \frac{3}{4}\, \mathrm{osc}_\ell(d)^2.
\end{aligned}$$

Finally, we consider the boundary edge $c := A \cap \Gamma \in \mathcal{E}_\ell^\star$. In this case, there holds

$$o_\ell(c|A)^2 = (|A|/2)\, \|f\|^2_{L^2(A_1)} + (|A|/4)\, \|f\|^2_{L^2(A_3)} + (|A|/4)\, \|f - f_A\|^2_{L^2(A)} \le \frac{3}{4}\, \mathrm{osc}_\ell(c)^2,$$

and we also observe the contraction property.

Having obtained (27)–(28), we may proceed as follows: We note that (26) provides

$$\begin{aligned}
\sum_{E \in \mathcal{E}_{\ell+1}^\star} \mathrm{osc}_{\ell+1}(E)^2 = \sum_{T \in \mathcal{T}_\ell} \sum_{\substack{E \in \mathcal{E}_{\ell+1}^\star \\ |T \cap \Omega_{\ell+1,E}| > 0}} \mathrm{osc}_{\ell+1}(E|T)^2 &\le \sum_{T \in \mathcal{T}_\ell} \sum_{\substack{E \in \mathcal{E}_\ell^\star \\ E \subset \partial T}} o_\ell(E|T)^2 \\
&= \sum_{E \in \mathcal{E}_\ell^\star} \sum_{\substack{T \in \mathcal{T}_\ell \\ T \subset \Omega_{\ell,E}}} o_\ell(E|T)^2.
\end{aligned}$$

Therefore, (27)–(28) show

$$\begin{aligned}
\sum_{E \in \mathcal{E}_{\ell+1}^\star} \mathrm{osc}_{\ell+1}(E)^2 &\le \sum_{E \in \mathcal{E}_\ell^\star \cap \mathcal{E}_{\ell+1}^\star} \mathrm{osc}_\ell(E)^2 + \frac{3}{4} \sum_{E \in \mathcal{E}_\ell^\star \setminus \mathcal{E}_{\ell+1}^\star} \mathrm{osc}_\ell(E)^2 \\
&= \sum_{E \in \mathcal{E}_\ell^\star} \mathrm{osc}_\ell(E)^2 - \frac{1}{4} \sum_{E \in \mathcal{E}_\ell^\star \setminus \mathcal{E}_{\ell+1}^\star} \mathrm{osc}_\ell(E)^2
\end{aligned}$$

Observing that $\mathcal{E}_\ell^\star \cap \mathcal{M}_\ell \subseteq \mathcal{E}_\ell^\star \setminus \mathcal{E}_{\ell+1}^\star$, we conclude the proof. $\square$

Proof of Proposition 3. First, the triangle inequality in the sequence space ℓ_2 proves

$$\begin{aligned}
\mu_{\ell+1} &= \Big(\sum_{T' \in \mathcal{T}_{\ell+1,\Gamma}} \mathrm{osc}_{\ell+1}(T')^2 + \sum_{E' \in \mathcal{E}_{\ell+1}^\star} \mathrm{osc}_{\ell+1}(E')^2 + \sum_{E' \in \mathcal{E}_{\ell+1}} h_{E'}\, \|[\partial_n U_{\ell+1}]\|^2_{L^2(E')} \Big)^{1/2} \\
&\le \Big(\sum_{T' \in \mathcal{T}_{\ell+1,\Gamma}} \mathrm{osc}_{\ell+1}(T')^2 + \sum_{E' \in \mathcal{E}_{\ell+1}^\star} \mathrm{osc}_{\ell+1}(E')^2 + \sum_{E' \in \mathcal{E}_{\ell+1}} h_{E'}\, \|[\partial_n U_\ell]\|^2_{L^2(E')} \Big)^{1/2} \\
&\quad + \Big(\sum_{E' \in \mathcal{E}_{\ell+1}} h_{E'}\, \|[\partial_n (U_{\ell+1} - U_\ell)]\|^2_{L^2(E')} \Big)^{1/2}.
\end{aligned}$$

In particular, the Young inequality proves for arbitrary $\delta > 0$

$$\begin{aligned}\mu_{\ell+1}^2 \le (1+\delta)\Big(\sum_{T'\in\mathcal{T}_{\ell+1,\Gamma}} \mathrm{osc}_{\ell+1}(T')^2 + \sum_{E'\in\mathcal{E}_{\ell+1}^\star} \mathrm{osc}_{\ell+1}(E')^2 + \sum_{E'\in\mathcal{E}_{\ell+1}} h_{E'}\,\|[\partial_n U_\ell]\|_{L^2(E')}^2\Big)\\ + (1+\delta^{-1}) \sum_{E'\in\mathcal{E}_{\ell+1}} h_{E'}\,\|[\partial_n (U_{\ell+1}-U_\ell)]\|_{L^2(E')}^2.\end{aligned} \tag{29}$$

Second, we use the estimates (23), (24), and (25) to see

$$\begin{aligned}&\sum_{T'\in\mathcal{T}_{\ell+1,\Gamma}} \mathrm{osc}_{\ell+1}(T')^2 + \sum_{E'\in\mathcal{E}_{\ell+1}^\star} \mathrm{osc}_{\ell+1}(E')^2 + \sum_{E'\in\mathcal{E}_{\ell+1}} h_{E'}\,\|[\partial_n U_\ell]\|_{L^2(E')}^2\\
&\le \sum_{T\in\mathcal{T}_{\ell,\Gamma}} \mathrm{osc}_\ell(T)^2 + \sum_{E\in\mathcal{E}_\ell^\star} \mathrm{osc}_\ell(E)^2 + \sum_{E'\in\mathcal{E}_\ell} h_E\,\|[\partial_n U_\ell]\|_{L^2(E)}^2\\
&\quad - \frac12 \sum_{T\in\mathcal{T}_{\ell,\Gamma}\cap\mathcal{M}_\ell} \mathrm{osc}_\ell(T)^2 - \frac14 \sum_{E\in\mathcal{E}_\ell^\star\cap\mathcal{M}_\ell} \mathrm{osc}_\ell(E)^2 - \frac12 \sum_{E'\in\mathcal{E}_\ell\cap\mathcal{M}_\ell} h_E\,\|[\partial_n U_\ell]\|_{L^2(E)}^2\\
&\le \mu_\ell^2 - \frac14\Big(\sum_{T\in\mathcal{T}_{\ell,\Gamma}\cap\mathcal{M}_\ell} \mathrm{osc}_\ell(T)^2 + \sum_{E\in\mathcal{E}_\ell^\star\cap\mathcal{M}_\ell} \mathrm{osc}_\ell(E)^2 + \sum_{E'\in\mathcal{E}_\ell\cap\mathcal{M}_\ell} h_E\,\|[\partial_n U_\ell]\|_{L^2(E)}^2\Big).\end{aligned}$$

Third, the Dörfler marking (21) yields

$$\begin{aligned}\sum_{T'\in\mathcal{T}_{\ell+1,\Gamma}} \mathrm{osc}_{\ell+1}(T')^2 + \sum_{E'\in\mathcal{E}_{\ell+1}^\star} \mathrm{osc}_{\ell+1}(E')^2 + \sum_{E'\in\mathcal{E}_{\ell+1}} h_{E'}\,\|[\partial_n U_\ell]\|_{L^2(E')}^2\\
\le (1-\theta/4)\mu_\ell^2.\end{aligned}$$

Fourth, according to uniform shape regularity of the generated family $(\mathcal{T}_\ell)_{\ell\in\mathbb{N}}$, there holds

$$\sum_{E'\in\mathcal{E}_{\ell+1}} h_{E'}\,\|[\partial_n (U_{\ell+1}-U_\ell)]\|_{L^2(E')}^2 \lesssim \|\nabla(U_{\ell+1}-U_\ell)\|_{L^2(\Omega)}^2 = |||U_{\ell+1}-U_\ell|||^2$$

Plugging the last two estimates into (29), we prove (22), where we finally choose $\delta > 0$ sufficiently small to guarantee $q := (1+\delta)(1-\theta/4) < 1$. □

Remark. *Clearly, Lemma 4 and 5 also hold if certain elements $T \in \mathcal{T}_\ell$ are refined by five bisections, as is done in* [6]*, or by so-called red-refinement. We refer to* [23, Chapter 4] *for details on different local mesh-refinements.*

The same holds for Lemma 6 as well. In case of bisec$_5$-refinement this is easily seen as follows: We theoretically build an intermediate mesh $\widetilde{\mathcal{T}}_{\ell+1}$, where elements marked for bisec$_5$ are refined by three bisections. Then, Lemma 6 applies for the refinement from $\mathcal{T}_\ell$ to $\widetilde{\mathcal{T}}_{\ell+1}$. To obtain $\mathcal{T}_{\ell+1}$, certain elements $T' \in \widetilde{\mathcal{T}}_{\ell+1}$ have to be refined by bisection. Since (25) *states, in particular, monotone decay of the oscillations, we conclude*

$$\mathrm{osc}_{\ell+1}^2 \le \widetilde{\mathrm{osc}}_{\ell+1}^2 \le \sum_{E\in\mathcal{E}_\ell^\star} \mathrm{osc}_\ell(E)^2 - \frac14 \sum_{E\in\mathcal{E}_\ell^\star\cap\mathcal{M}_\ell} \mathrm{osc}_\ell(E)^2.$$

Finally, if certain elements of $\mathcal{T}_\ell$ are refined by red-refinement, the proof of (25) *is obtained by similar elementary calculations as in the proof of Lemma 6. We refer to* [21] *for details.* □

Remark. *Under further assumptions, the same analysis can be used to prove the estimator reduction of Proposition 3 for* η_ℓ *instead of* μ_ℓ*. For given* $\theta \in (0,1)$*, let* $\mathcal{M}_\ell \subseteq \mathcal{E}_\ell \cup \mathcal{T}_{\ell,\Gamma}$ *satisfy*

$$\theta\, \eta_\ell^2 \le \sum_{E \in \mathcal{E}_\ell \cap \mathcal{M}_\ell} \big(\eta_\ell(E)^2 + \mathrm{osc}_\ell(E)^2\big) + \sum_{T \in \mathcal{T}_{\ell,\Gamma} \cap \mathcal{M}_\ell} \mathrm{osc}_\ell(T)^2. \tag{30}$$

First, suppose that each element $T \in \mathcal{T}_\ell$ *has at most one edge on the boundary* Γ*. This can be guaranteed, for instance, by certain refinement of elements* $T \in \mathcal{T}_0$ *in the initial mesh. Let* $\mathcal{T}_{\ell,\Gamma}^\star := \big\{T \in \mathcal{T}_{\ell,\Gamma} \,:\, |T \cap \Gamma| = 0\big\}$ *denote the set of elements, which have some node on* Γ*, but no edge. Note that —according to the assumption on the mesh— there is a one-to-one correspondence of the elements with edge on the boundary* $\mathcal{T}_{\ell,\Gamma} \backslash \mathcal{T}_{\ell,\Gamma}^\star$ *and the boundary edges* $\mathcal{E}_{\ell,\Gamma} = \mathcal{E}_\ell^\star \backslash \mathcal{E}_\ell$*. Therefore, the error estimator* η_ℓ *can be rewritten in the form*

$$\eta_\ell^2 = \sum_{E \in \mathcal{E}_\ell} \eta_\ell(E)^2 + \sum_{E \in \mathcal{E}_\ell^\star} \mathrm{osc}_\ell(E)^2 + \sum_{T \in \mathcal{T}_{\ell,\Gamma}^\star} \mathrm{osc}_\ell(T)^2,$$

and the set $\mathcal{M}_\ell$ *can be interpreted as some set* $\mathcal{M}_\ell^\star \subseteq \mathcal{E}_\ell^\star \cup \mathcal{T}_{\ell,\Gamma}^\star$ *with*

$$\theta\, \eta_\ell^2 \le \sum_{E \in \mathcal{E}_\ell \cap \mathcal{M}_\ell^\star} \eta_\ell(E)^2 + \sum_{E \in \mathcal{E}_\ell^\star \cap \mathcal{M}_\ell^\star} \mathrm{osc}_\ell(E)^2 + \sum_{T \in \mathcal{T}_{\ell,\Gamma}^\star \cap \mathcal{M}_\ell^\star} \mathrm{osc}_\ell(T)^2.$$

However, if $T \in \mathcal{T}_{\ell,\Gamma} \cap \mathcal{M}_\ell$ *with* $|T \cap \Gamma| > 0$ *is marked for refinement, so far, only its reference edge is refined. Therefore, the actual refinement rule does not guarantee that the edge* $E = T \cap \Gamma \in \mathcal{E}_\ell^\star \backslash \mathcal{E}_\ell$ *is split. Put differently, the actual refinement rule does not guarantee that all edges* $E \in \mathcal{E}_\ell^\star \cap \mathcal{M}_\ell^\star$ *are refined. One remedy is that marked elements* $T \in \mathcal{T}_{\ell,\Gamma} \cap \mathcal{M}_\ell$ *are refined (at least) by three bisections (or by red-refinement). With this convention, all edges* $E \in \mathcal{E}_\ell^\star \cap \mathcal{M}_\ell^\star$ *are refined. Therefore, Lemma 5 and Lemma 6 apply. Moreover, the proof of Lemma 4 carries over if* $\mathcal{T}_{\ell,\Gamma}$ *is replaced by* $\mathcal{T}_{\ell,\Gamma}^\star$*. Altogether, this proves that the Dörfler marking* (30) *and the extended refinement strategy guarantee*

$$\eta_{\ell+1}^2 \le q\, \eta_\ell^2 + C_2 |||U_{\ell+1} - U_\ell|||^2 \tag{31}$$

with some contraction constant $q \in (0,1)$ *which depends only on* $\theta \in (0,1)$ *and the same constant* $C_2 > 0$ *as in Proposition 3.* □

3.2. Convergent Adaptive Algorithm. In this section, we formally state our version of the adaptive algorithm and prove that it generates a sequence of discrete solutions U_ℓ which converge to the continuous minimizer u.

Algorithm 7. *Fix* $0 < \theta < 1$ *and let* $\mathcal{T}_\ell$ *with* $\ell = 0$ *be the initial triangulation. For each* $\ell = 0, 1, 2, \dots$ *do:*

- (i) *Compute discrete solution* $U_\ell \in \mathcal{A}_\ell := \mathcal{A} \cap \mathcal{S}^1(\mathcal{T}_\ell)$
- (ii) *Compute indicators* $\eta_\ell(E)^2 + \mathrm{osc}_\ell(E)^2$ *and* $\mathrm{osc}_\ell(T)^2$ *for all* $E \in \mathcal{E}_\ell$ *and all* $T \in \mathcal{T}_{\ell,\Gamma}$*.*
- (iii) *Determine set* $\mathcal{M}_\ell \subseteq \mathcal{E}_\ell \cup \mathcal{T}_{\ell,\Gamma}$ *which satisfies*

$$\theta\, \eta_\ell^2 \le \sum_{E \in \mathcal{E}_\ell \cap \mathcal{M}_\ell} \big(\eta_\ell(E)^2 + \mathrm{osc}_\ell(E)^2\big) + \sum_{T \in \mathcal{T}_{\ell,\Gamma} \cap \mathcal{M}_\ell} \mathrm{osc}_\ell(T)^2. \tag{32}$$

- (iv) *Mark all edges* $E \in \mathcal{E}_\ell \cap \mathcal{M}_\ell$ *and all reference edges of* $T \in \mathcal{T}_{\ell,\Gamma} \cap \mathcal{M}_\ell$ *for refinement.*
- (v) *Obtain new mesh* $\mathcal{T}_{\ell+1}$ *by newest vertex bisection and increase counter* $\ell \mapsto \ell + 1$*.*

Theorem 8. *Let μ_ℓ denote the error estimator introduced in Section 3.1 and suppose that, nevertheless, η_ℓ is used for marking (32) in Algorithm 7. Then, Algorithm 7 guarantees that the combined error quantity*

$$\Delta_\ell := \mathcal{J}(U_\ell) - \mathcal{J}(u) + \gamma\,\mu_\ell^2 \tag{33}$$

satisfies the contraction property

$$\Delta_{\ell+1} \le \kappa\,\Delta_\ell \quad \textit{for all } \ell \in \mathbb{N}. \tag{34}$$

The constants $0 < \gamma, \kappa < 1$ depend only on the parameter θ and the shape of the elements in $\mathcal{T}_0$. In particular, there holds $\lim_{\ell\to\infty} \mathcal{J}(U_\ell) = \mathcal{J}(u)$ as well as $\lim_{\ell\to\infty} |||u - U_\ell||| = 0 = \lim_{\ell\to\infty} \eta_\ell$.

Proof. Note that the equivalence (20) of η_ℓ and μ_ℓ and the Dörfler marking (32) for η_ℓ provide

$$\frac{\theta}{4}\,\mu_\ell^2 \le \theta\,\eta_\ell^2 \le \sum_{E\in\mathcal{E}_\ell\cap\mathcal{M}_\ell} \big(\eta_\ell(E)^2 + \mathrm{osc}_\ell(E)^2\big) + \sum_{T\in\mathcal{T}_{\ell,\Gamma}\cap\mathcal{M}_\ell} \mathrm{osc}_\ell(T)^2.$$

Consequently, $\mathcal{M}_\ell$ satisfies the Dörfler marking (21) for μ_ℓ with modified parameter $\widetilde{\theta} = \theta/4 \in (0,1)$. According to Proposition 3, this implies

$$\mu_{\ell+1}^2 \le q\,\mu_\ell^2 + C_2\,|||U_{\ell+1} - U_\ell|||^2$$

with certain constants $0 < q < 1$ and $C_2 > 0$. Therefore,

$$\begin{aligned}\Delta_{\ell+1} &= \mathcal{J}(U_\ell) - \mathcal{J}(u) + \gamma\,\mu_{\ell+1}^2 - \big(\mathcal{J}(U_\ell) - \mathcal{J}(U_{\ell+1})\big)\\ &\le \mathcal{J}(U_\ell) - \mathcal{J}(u) + \gamma q\,\mu_\ell^2 + \gamma C_2\,|||U_{\ell+1} - U_\ell|||^2 - \big(\mathcal{J}(U_\ell) - \mathcal{J}(U_{\ell+1})\big).\end{aligned}$$

Using the variational inequality (11) applied for $U_{\ell+1}$, we proceed as in the proof of Proposition 2 to see

$$\frac{1}{2}\,|||U_{\ell+1} - U_\ell|||^2 \le \mathcal{J}(U_\ell) - \mathcal{J}(U_{\ell+1})$$

Choosing γ sufficiently small to guarantee $\gamma C_2 - 1/2 \le 0$, we then obtain

$$\Delta_{\ell+1} \le \mathcal{J}(U_\ell) - \mathcal{J}(u) + \gamma q\,\mu_\ell^2 + (\gamma C_2 - 1/2)\,|||U_{\ell+1} - U_\ell|||^2 \le \mathcal{J}(U_\ell) - \mathcal{J}(u) + \gamma q\,\mu_\ell^2.$$

According to Proposition 2 and equivalence (20) of η_ℓ and μ_ℓ, there holds

$$C_1^{-1}\,\big(\mathcal{J}(U_\ell) - \mathcal{J}(u)\big) \le \eta_\ell^2 \le \mu_\ell^2.$$

For $\varepsilon > 0$, we thus observe

$$\mathcal{J}(U_\ell) - \mathcal{J}(u) + \gamma q\,\mu_\ell^2 \le (1 - \gamma\varepsilon C_1^{-1})\big(\mathcal{J}(U_\ell) - \mathcal{J}(u)\big) + \gamma(q+\varepsilon)\mu_\ell^2 \le \kappa\,\Delta_\ell \tag{35}$$

with $\kappa := \max\{1 - \gamma\varepsilon C_2^{-1}, q + \varepsilon\}$. Since $q < 1$, we may choose $\varepsilon > 0$ sufficiently small to guarantee $q + \varepsilon < 1$. This choice leads to $\kappa < 1$, and we finally end up with (34). By induction, this implies

$$\lim_{\ell\to\infty} \Delta_\ell = 0, \quad \text{whence} \quad \lim_{\ell\to\infty} \mathcal{J}(U_\ell) = \mathcal{J}(u) \text{ and } \lim_{\ell\to\infty} \mu_\ell = 0.$$

With the estimate $\eta_\ell \le \mu_\ell$ and reliability $|||u - U_\ell||| \lesssim \eta_\ell$, we thus conclude the proof. $\square$

In [6], the weighting $h_T^2 = \mathrm{diam}(T)^2$ instead of $|T|$ is used in the definition (16) of $\mathrm{osc}_\ell(T)$, i.e.,

$$\widetilde{\eta}_\ell^2 := \sum_{E\in\mathcal{E}_\ell} \big(\eta_\ell(E)^2 + \mathrm{osc}_\ell(E)^2\big) + \sum_{T\in\mathcal{T}_{\ell,\Gamma}} \widetilde{\mathrm{osc}}_\ell(T)^2, \tag{36}$$

where

$$\widetilde{\mathrm{osc}}_\ell(T)^2 = h_T^2\,\|f\|_{L^2(T)}^2 \quad \text{for } T\in\mathcal{T}_{\ell,\Gamma}. \tag{37}$$

Note that this definition does not necessarily yield a contraction $h_{T'} < h_T$ if an element $T\in\mathcal{T}_{\ell,\Gamma}\cap\mathcal{M}_\ell$ is refined and $T'\in\mathcal{T}_{\ell+1}$ is one of the resulting sons. Nevertheless, $\widetilde{\eta}_\ell$ leads to a convergent adaptive FEM in the sense of Theorem 8.

Corollary 9. *Suppose that $\widetilde{\eta}_\ell$ instead of η_ℓ is used in Algorithm 7 for marking. Then, the modified algorithm still guarantees the contraction property* (34). *In particular, there holds $\lim_{\ell\to\infty}\mathcal{J}(U_\ell) = \mathcal{J}(u)$ as well as $\lim_{\ell\to\infty} |||u-U_\ell||| = 0 = \lim_{\ell\to\infty}\widetilde{\eta}_\ell$.*

Proof. Note that there holds

$$\mathrm{osc}_\ell(T) \le \widetilde{\mathrm{osc}}_\ell(T) \le C_3\,\mathrm{osc}_\ell(T) \quad \text{for all } T\in\mathcal{T}_{\ell,\Gamma} \tag{38}$$

with some constant $C_3 \ge 1$ which depends only on the shape regularity of the mesh $\mathcal{T}_\ell$. Since newest vertex bisection leads to uniformly shape regular meshes, C_3 may be chosen independently of ℓ. The Dörfler marking (32) for $\widetilde{\eta}_\ell$ thus implies

$$\begin{aligned}\theta\,\eta_\ell \le \theta\,\widetilde{\eta}_\ell &\le \sum_{E\in\mathcal{E}_\ell\cap\mathcal{M}_\ell} \big(\eta_\ell(E)^2 + \mathrm{osc}_\ell(E)^2\big) + \sum_{T\in\mathcal{T}_{\ell,\Gamma}\cap\mathcal{M}_\ell} \widetilde{\mathrm{osc}}_\ell(T)^2 \\ &\le C_3\Big(\sum_{E\in\mathcal{E}_\ell\cap\mathcal{M}_\ell} \big(\eta_\ell(E)^2 + \mathrm{osc}_\ell(E)^2\big) + \sum_{T\in\mathcal{T}_{\ell,\Gamma}\cap\mathcal{M}_\ell} \mathrm{osc}_\ell(T)^2\Big).\end{aligned}$$

Put differently, the set $\mathcal{M}_\ell$ satisfies the Dörfler marking (32) for $(\theta,\widetilde{\eta}_\ell)$ as well as the Dörfler marking (32) for $(\widetilde{\theta},\eta_\ell)$, where $\widetilde{\theta} = \theta/C_3 \in (0,1)$. Therefore, Theorem 8 applies and (34) holds. In particular, $\lim_{\ell\to\infty}\eta_\ell = 0$ and the equivalence (38) also conclude $\lim_{\ell\to\infty}\widetilde{\eta}_\ell = 0$. □

Remark. *Under the additional assumptions on the mesh-refinement, cf. the remark at the end of Section 3.1, one can prove contraction* (34) *of $\Delta_\ell := \mathcal{J}(U_\ell) - \mathcal{J}(u) + \gamma\,\eta_\ell^2$ in Theorem 8 and Corollary 9, where η_ℓ replaces μ_ℓ in the definition of Δ_ℓ.* □

Remark. *The estimator reduction* (22) *already implies convergence $\lim_\ell \mu_\ell = 0$, whence $\lim_\ell \mathcal{J}(U_\ell) = \mathcal{J}(u)$ as well as $\lim_\ell |||u-U_\ell||| = 0$ according to Proposition 2. To see this, it remains to verify that the obstacle problem leads to* a priori convergence $\lim_\ell U_\ell = u_\infty$ *with a certain limit $u_\infty\in\mathcal{H}$. For linear problems, such a result is found in* [1, 11, 19], *and we refer to* [21] *for the proof of the a priori convergence in our non-linear setting. Then,* (22) *takes the form*

$$\mu_{\ell+1}^2 \le q\,\mu_\ell^2 + \alpha_\ell$$

with the zero sequence $\alpha_\ell = C_2\,|||U_{\ell+1} - U_\ell|||^2 \ge 0$. Therefore, elementary calculus concludes $\lim_\ell \mu_\ell = 0$, *cf.* [1]. *We stress that, contrary to* [19], *the estimator reduction concept from* [1] *avoids any use of discrete efficiency. It is only based on the precise definition of the error* *estimator, a uniform decay of the mesh-width locally on marked elements, and the observation that any kind of mesh-refinement will lead to a convergent sequence of discrete solutions. We stress, however, that the convergence results in Theorem 8 and Corollary 9 are stronger since they include even a contraction of some error quantity* $\Delta_\ell \geq \varepsilon_\ell = \mathcal{J}(U_\ell) - \mathcal{J}(u)$. □

ℓ	N	$\sqrt{\varepsilon_\ell}$	η_ℓ	osc_ℓ
1	38	9.6584e-01	7.8592e+00	7.6804e+00
2	70	5.7088e-01	4.4866e+00	4.1953e+00
3	156	3.8544e-01	2.6368e+00	2.2612e+00
4	316	3.4255e-01	1.6397e+00	1.1892e+00
5	568	2.1016e-01	1.0907e+00	7.1523e-01
6	1088	1.4429e-01	7.2078e-01	3.9564e-01
7	1966	9.8835e-02	4.9444e-01	2.1653e-01
8	3524	6.9485e-02	3.4353e-01	1.3578e-01
9	6438	4.8982e-02	2.4228e-01	7.6460e-02
10	12270	3.3545e-02	1.6831e-01	4.3110e-02
11	22140	2.3780e-02	1.2136e-01	2.5694e-02
12	42620	1.6327e-02	8.5847e-02	1.4742e-02
13	77918	1.0873e-02	6.2456e-02	9.6058e-03
14	146854	8.6766e-03	4.4498e-02	5.3497e-03
15	268400	6.0689e-03	3.2346e-02	4.4724e-03
16	491250	4.1792e-03	2.3719e-02	2.4099e-03
17	925574	2.8772e-03	1.7260e-02	1.5729e-03

Table 1. Numerical results for adaptive mesh-refinement with $\theta = 0.6$, where $N = \#\mathcal{T}_\ell$, $\varepsilon_\ell = \mathcal{J}(U_\ell) - \mathcal{J}(u)$, and osc_ℓ from (43).

4. Numerical Experiment

In this section, we consider a numerical experiment from [6]. The conforming and shape regular mesh is adaptively generated by Algorithm 7. For the solution of the discrete obstacle problem at each level, the primal-dual active set strategy from [15] has been used. For the initial mesh $\mathcal{T}_0$, we choose $(U_0^{(0)}, \lambda_0^{(0)}) \equiv (0,0)$ for the primal dual pair as initial guesses for the iterative solver. For $\mathcal{T}_\ell$, we choose the prolongated discrete solutions associated with the previous mesh, i.e., $U_\ell^{(0)} := U_{\ell-1}$ as well as $\lambda_\ell^{(0)} := \lambda_{\ell-1}$. We stop the iterative solver if the difference of two consecutive solutions satisfies

$$\|\!|U_\ell^{(j)} - U_\ell^{(j-1))}|\!\| \leq \tau\, N^{-1/2} \tag{39}$$

for some tolerance $\tau > 0$, where $N = \#\mathcal{T}_\ell$ denotes the number of elements. We then define our discrete solution at $\mathcal{T}_\ell$ by $U_\ell := U_\ell^{(j)}$ and $\lambda_\ell := \lambda_\ell^{(j)}$.

While the numerical results are quite similar to those in [6], we stress that our approach theoretically includes the data oscillations into the estimator η_ℓ.

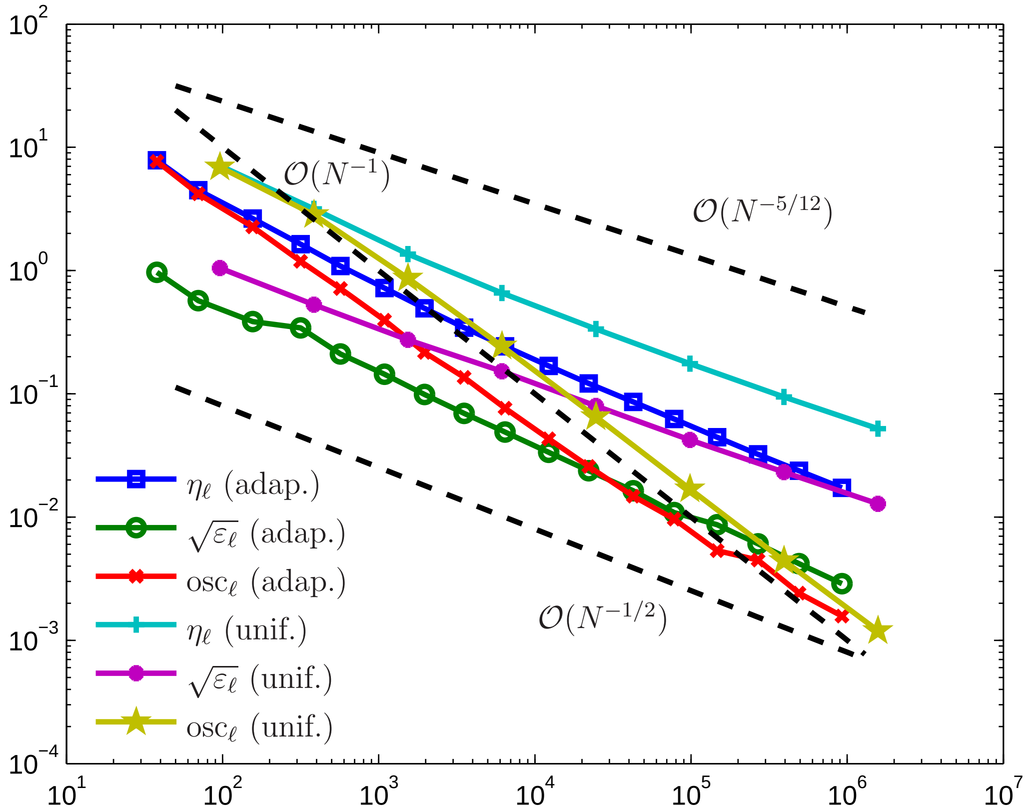

FIGURE 4. Numerical results for uniform and adaptive mesh-refinement with $\theta = 0.6$, where $\varepsilon_\ell = \mathcal{J}(U_\ell) - \mathcal{J}(u)$, η_ℓ, and osc_ℓ are plotted over the number $N = \#\mathcal{T}_\ell$ of elements.

We consider the obstacle problem with constant obstacle $\chi \equiv 0$ on the L-shaped domain $\Omega := (-2,2)^2 \setminus [0,2) \times (-2,0]$. The right-hand side is given in polar coordinates by

$$f(r,\varphi) := -r^{2/3}\sin(2\varphi/3)\big(\gamma_1'(r)/r + \gamma_1''(r)\big) - \frac{4}{3}r^{-1/3}\gamma_1'(r)\sin(2\varphi/3) - \gamma_2(r), \tag{40}$$

where $(\cdot)'$ denotes the radial derivative d/dr. Moreover, $\bar r := 2(r - 1/4)$ and

$$\gamma_1(r) = \begin{cases} 1, & \bar r < 0, \\ -6\bar r^5 + 15\bar r^4 - 10\bar r^3 + 1, & 0 \le \bar r < 1, \\ 0, & \bar r \ge 1, \end{cases}$$

$$\gamma_2(r) = \begin{cases} 0, & r \le 5/4, \\ 1, & \text{else.} \end{cases}$$

Then, the exact solution reads in polar coordinates

$$u(r,\varphi) = r^{2/3}\gamma_1(r)\sin(2\varphi/3) \tag{41}$$

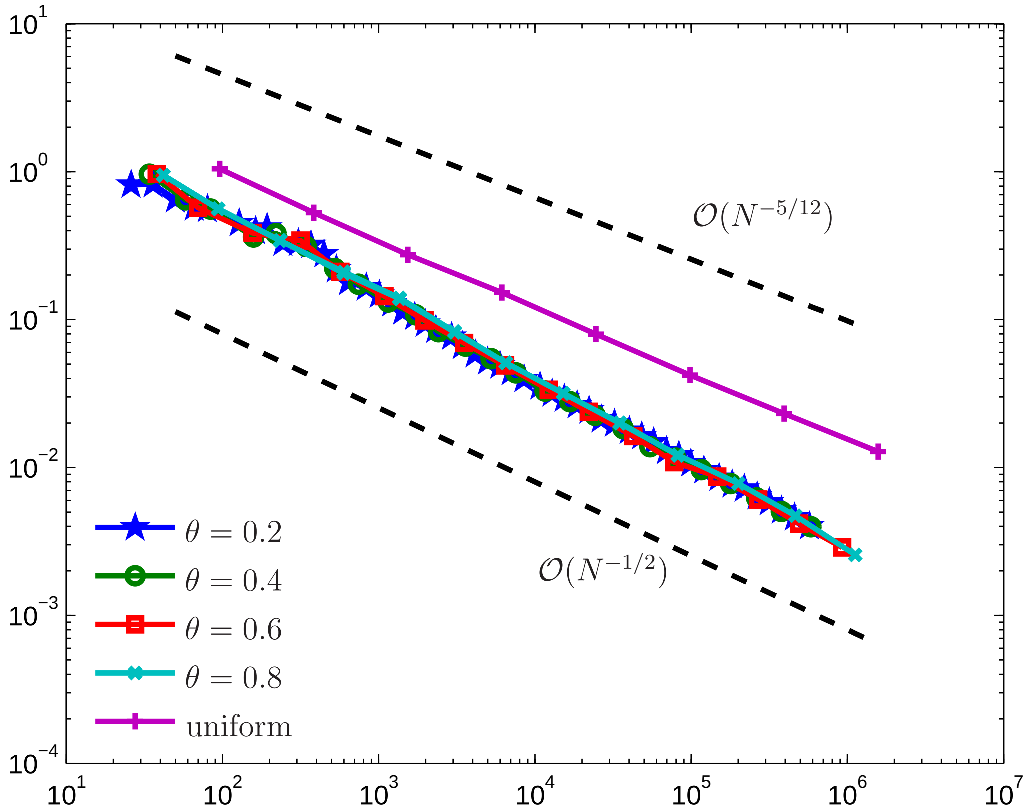

FIGURE 5. Numerical results for $\sqrt{\varepsilon_\ell}$ for uniform and adaptive mesh-refinement with $\theta \in \{0.2, 0.4, 0.6, 0.8\}$, plotted over the number $N = \#\mathcal{T}_\ell$ of elements.

and exhibits a corner singularity at the origin. We compare uniform and adaptive mesh-refinement, where we vary the adaptivity parameter $\theta \in \{0.2, 0.4, 0.6, 0.8\}$ in Algorithm 7.

Table 1 provides the experimental results for adaptive mesh-refinement with $\theta = 0.6$, where the energy error reads

$$\varepsilon_\ell = \mathcal{J}(U_\ell) - \mathcal{J}(u), \tag{42}$$

the overall data oscillations are defined by

$$\mathrm{osc}_\ell^2 = \sum_{E \in \mathcal{E}_\ell} \mathrm{osc}_\ell(E)^2 + \sum_{T \in \mathcal{T}_{\ell,\Gamma}} \mathrm{osc}_\ell(T)^2, \tag{43}$$

and the error estimator η_ℓ, defined in (13), includes oscillations and edge jumps.

In Figure 4, we plot $\sqrt{\varepsilon_\ell}$, η_ℓ, and osc_ℓ over the number $N = \#\mathcal{T}_\ell$ of elements for uniform and adaptive mesh-refinement with $\theta = 0.6$. Uniform mesh-refinement leads to a suboptimal convergence behaviour $\sqrt{\varepsilon_\ell} \approx \mathcal{O}(N^{-5/12})$ with respect to the number $N = \#\mathcal{T}_\ell$ of elements. Contrary, adaptive mesh-refinement regains the optimal order of convergence $\sqrt{\varepsilon_\ell} = \mathcal{O}(N^{-1/2})$. We stress that the given data are smooth so that uniform as well as

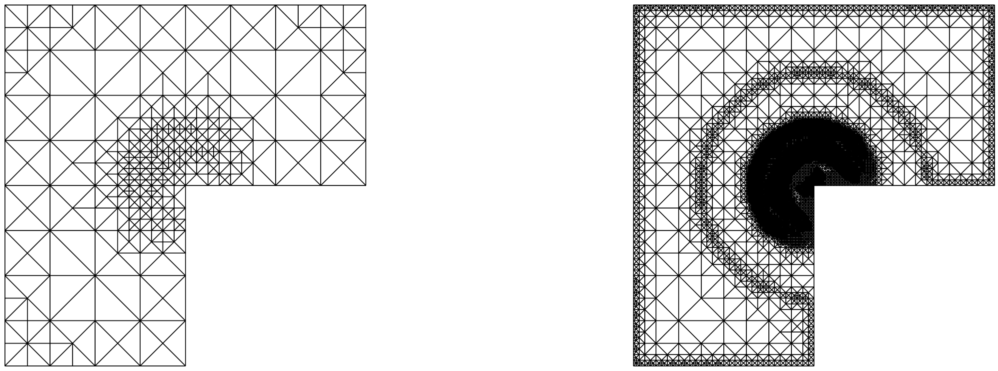

FIGURE 6. Adaptively generated meshes $\mathcal{T}_5$ (*left*) and $\mathcal{T}_{11}$ (*right*) with $N = 568$ and $N = 22140$ elements, respectively, for $\theta = 0.6$.

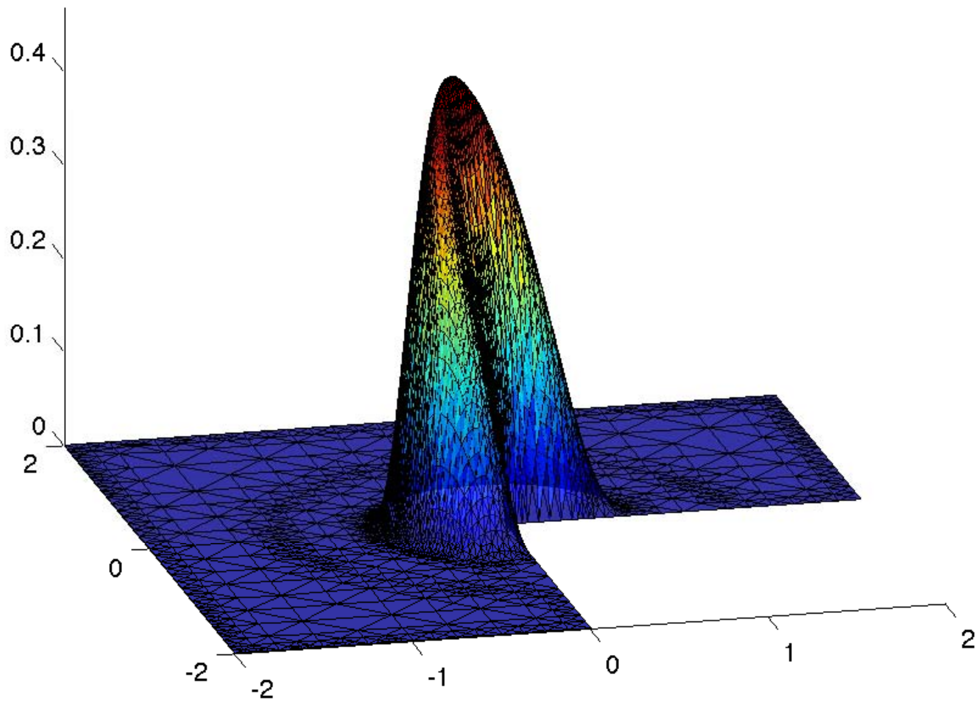

FIGURE 7. Galerkin solution U_8 on adaptively generated mesh $\mathcal{T}_8$ with $N = 3524$ elements for $\theta = 0.6$.

adaptive mesh-refinement leads to $\mathrm{osc}_\ell = \mathcal{O}(N^{-1})$, which corresponds to second-order convergence with respect to a uniform mesh-width. For both mesh-refinements, we see that the curves of η_ℓ and $\sqrt{\varepsilon_\ell}$ are parallel. This experimentally confirms the reliability of η_ℓ from Proposition 2 and indicates that η_ℓ is also efficient.

Figure 5 provides the experimental comparison for different values of $\theta \in \{0.2, 0.4, 0.6, 0.8\}$. We see that each choice of θ leads to optimal order of convergence and that the corresponding curves essentially coincide. Since achievement of a prescribed precision takes much longer with uniform refinement, the benefits of adaptive refinement are clearly visible. Additionally, we stress that also the convergence rate itself is improved.

Figure 6 displays the adaptively generated meshes $\mathcal{T}_5$ and $\mathcal{T}_{11}$, respectively for $\theta = 0.6$. As expected, refinement is basically restricted to the inactive zone. Due to the data oscillation terms in the estimator η_ℓ —and hence contrary to [6]— we also observe certain refinement within the active zone. Finally, Figure 7 shows the discrete solution on $\mathcal{T}_8$.

References

[1] M. Aurada, S. Ferraz-Leite, D. Praetorius: *Estimator reduction and convergence of adaptive FEM and BEM*, ASC Report **27/2009**, Institute for Analysis and Scientific Computing, Vienna University of Technology, Wien 2009.

[2] M. Ainsworth, T. Oden: *A posteriori error estimation in finite element analysis*, Wiley-Interscience, New-York, 2000.

[3] M. Ainsworth, C. Lee, T. Oden: *Local a posterori error estimators for variational inequalities*, Numer. Meth. Part. D. E. **9** (1993), 23–33.

[4] D. Braess: *A posteriori error estimators for obstacle problems — another look*, Numer. Math. **101** (2005), 415–421.

[5] S. Bartels, C. Carstensen: *Averaging techniques yield reliable a posteriori finite element error control for obstacle problems*, Numer. Math. **99** (2004), 225–249.

[6] D. Braess, C. Carstensen, R. Hoppe: *Convergence analysis of a conforming adaptive finite element method for an obstacle problem*, Numer. Math. **107** (2007), 455–471.

[7] D. Braess, C. Carstensen, R. Hoppe: *Error reduction in adaptive finite element approximations of elliptic obstacle problems*, J. Comput. Math. **27** (2009), 148–169.

[8] C. Carstensen, R. Hoppe: *Convergence analysis of an adaptive edge finite element method for the 2D eddy current equations*, J. Numer. Math. **13** (2005), 19–32.

[9] C. Carstensen, R. Hoppe: *Error reduction and convergence for an adaptive mixed finite element method*, Math. Comp. **75** (2006), 1033–1042.

[10] C. Carstensen, R. Hoppe: *Convergence analysis of an adaptive nonconforming finite element method*, Numer. Math. **103** (2006), 251–266.

[11] C. Carstensen, D. Praetorius: *Convergence of adaptive boundary element methods*, ASC Report **15/2009**, Institute for Analysis and Scientific Computing, Vienna University of Technology, Wien 2009.

[12] J. Cascon, C. Kreuzer, R. Nochetto, K, Siebert: *Quasi-optimal convergence rate for an adaptive finite element method*, SIAM J. Numer. Anal. **46** (2008), 2524–2550.

[13] Z. Chen, R. Nochetto: *Residual type a posteriori error estimates for elliptic obstacle problems*, Numer. Math. **84** (2000), 527–548.

[14] W. Dörfler: *A convergent adaptive algorithm for Poisson's equation*, SIAM J. Numer. Anal. **33** (1996), 1106–1124.

[15] M. Hintermüller, K. Ito, K. Kunisch: *The primal-dual active set strategy as a semismooth newton method*, SIAM J. Optim., **13** (2003), 865–888.

[16] D. Kinderlehrer, G. Stampacchia: *An introduction to variational inequalities*, Academic Press, New York, 1980.

[17] W. Liu, N. Yan: *A posteriori error estimates for a class of variational inequalities*, J. Sci. Comput. **15** (2000), 361–393.

[18] P. Morin, R. Nochetto, K. Siebert: *Data oscillation and convergence of adaptive FEM*, SIAM. J. Numer. Anal.. **18** (2000), 466–488.

[19] P. Morin, K. Siebert, A. Veeser: *A basic convergence result for conforming adaptive finite elements*, Math. Models Methods Appl. Sci. **18** (2008), 707–737.

[20] R. Nochetto, K. Siebert, A. Veeser: *Fully localized a posteriori error estimators and barrier sets for contact problems*, SIAM J. Numer. Anal. **42** (2005), 2118–2135.

[21] M. Page: *Schätzerreduktion und Konvergenz adaptiver FEM für Hindernisprobleme*, Master thesis (in German), Institute for Analysis and Scientific Computing, Vienna University of Technology, Wien 2010.

[22] R. Stevenson: *Optimality of standard adaptive finite element method,* Found. Comput. Math. (2007), 245–269.

[23] R. Verfürth: *A review of a posteriori error estimation and adaptive mesh-refinement techniques*, Wiley-Teubner, 1996.

[24] A. Veeser: *Efficient and reliable a posteriori error estimators for elliptic obstacle problems*, SIAM J. Numer. Anal. **39** (2001), 146–167.

[25] A. Veeser: *Convergent adaptive finite elements for the nonlinear Laplacian*, Numer. Math. **92** (2002), 743–770.

Institute for Analysis and Scientific Computing, Vienna University of Technology, Wiedner Hauptstrasse 8-10, A-1040 Wien, Austria

E-mail address: `Marcus.Page@gmx.de`

E-mail address: `Dirk.Praetorius@tuwien.ac.at` (corresponding author)